Parallel Chirality Inductions in Möbius Zn(II) Hexaphyrin Transformation Networks

Thomas Nédellec, Bernard Boitrel, Stéphane Le Gac

Parallel Chirality Inductions in Möbius Zn(II) Hexaphyrin Transformation Networks

Thomas Nédellec, Bernard Boitrel and Stéphane Le Gac*

Univ Rennes, CNRS, ISCR (Institut des Sciences Chimiques de Rennes)-UMR 6226, 35000 Rennes (France)

ABSTRACT: Networked chemical transformations are key features of biological systems, in which complex multi-component interactions enable the emergence of sophisticated functions. Being interested in chirality induction phenomena with dynamic Möbius π-systems, we have designed a pair of Möbius [28]hexaphyrin ligands in order to investigate mixtures rather than isolated molecules. Thus, an hexaphyrin bearing a chiral amino arm was first optimized and found to bind a ZnOAc moiety, triggering an impressive quasi-quantitative chirality induction over the Möbius π-system. Secondly, this amino-type hexaphyrin was mixed with a second hexaphyrin bearing a chiral carboxylate arm, affording at first ill-defined coordination assemblies in the presence of zinc. In contrast, a social self-sorting behavior occurred upon addition of two exogenous achiral effectors (AcO^- and $BuNH_2$), leading to a well-defined 1:1 mixture of two Möbius complexes featuring a sole Möbius twist configuration (parallel chirality inductions). We next successfully achieved a compartmentalized switching, *i.e.* a single-component transformation from such a complex mixture. The $BuNH_2$ effector was selectively protected with Boc_2O, owing to a lower reactivity of the arm's NH_2 function intramolecularly bound to zinc, and subsequent addition of $BuNH_2$ restored the initial mixture retaining parallel chirality inductions (five cycles). By changing the nature and twist configuration of only one of the two complexes, at initial state or by switching, this approach enables a 'two-channel' tuning of the chiroptical properties of the ensemble. Such multiple dynamic chirality inductions, controlled by selective metal-ligand recognition and chemical reactivity, set down the basis for Möbius-type stereoselective transformation networks with new functions.

Introduction

Expanded porphyrins have been scrutinized for several decades, revealing a dense family of macrocycles with intriguing structural, electronic and optical properties.[1] A striking difference with porphyrins, beyond three-dimensional structures such as figure eight or Möbius-type, lies in the magnified flexibility of enlarged poly-pyrrolic scaffolds affording plenty of possibilities to create dynamic shape-shifting entities. Various stimuli such as protonation, redox processes, solvent, temperature or metal ion coordination, have been used to trigger conformational rearrangements with notably a deep impact on the π-conjugation and aromaticity.[1h,j] Despite these advances, the significance of expanded porphyrins as responsive sub-units of larger molecular architectures, able to generate and control new properties and functions, has been considered only recently.[2] The research fields of allosteric receptors and catalysts,[3] as well as of molecular switches and devices,[4] would certainly gain great advantages of the responsiveness of flexible porphyrinoids.[5] However, the lack of general approaches for the selective and efficient post-modification of larger porphyrinoids,[6] in relation to their somehow intrinsic and unpredictable reactivity, likely prevents such developments. Therefore, flexible expanded porphyrins fully deserve further investigations with the aim to identify dynamic platforms suitable to create innovative adaptive architectures and systems. Adaptive chemistry[7] is indeed a powerful notion reflecting the capacity of a programmed dynamic (supra)molecular system to evolve upon changes of the environment, enabling the emergence of sophisticated behaviors from complex transformation networks.[8]

In this regard, the regular hexaphyrin scaffold – the six-pyrrole homologue of porphyrins – holds great promises.[9] Among remarkable features,[1h,10] this porphyrinoid readily forms a Möbius aromatic 28-π system exhibiting a fluxional equilibrium between degenerate isomers (Figure 1a, left).[11,12,13] Consequently, the inherent chirality of this Möbius π system is dynamic, and a fast interconversion between *P* and *M* twist configurations occurs in solution at ambient temperature (energy barrier ~8 kcal/mol).[14] While this system can be frozen upon metal (*e.g.* group 10 metals)[15] or main group element (*e.g.* P, Si)[16] insertion, allowing in some cases separation of *P*/*M* enantiomers,[17] our group has been interested in labile Zn(II) coordination complexes leading to dynamic metallo-receptors formed under thermodynamic conditions, setting down the basis of adaptive behaviors.[18] This Möbius [28]hexaphyrin scaffold may further undergo other dynamic events (Figure 1a, right): (i) equilibrium between other conformations such as Hückel (planar) antiaromatic ones (rectangular, triangular, dumbbell);[1h] (ii) isomorphic equilibrium between degenerate isomers upon a 'four-pyrrole' inversion.[19]

Taken together, these dynamic features confer to the regular hexaphyrin scaffold the capacity to form virtual dynamic libraries of ligands and molecular hosts,[18e] and to participate in transformation networks when properly functionalized.[2b,18b] They further offer unique possibilities to study chirality induction phenomena at the level of the Möbius twist in changing environments.[18] Fine control over the stereoselective formation of Möbius stereoisomers has remained challenging[17] and, to the best of our knowledge, has not been described with other types of Möbius scaffolds. Interestingly, the chirality of the twisted π-system of hexaphyrins generates a marked Cotton effect in electronic circular dichroism (ECD) spectroscopy, in the red part of the visible spectrum.[17,18,20] *In fine*, tuning the chiroptical properties of Möbius π-systems may afford new opportunities in π-materials for technological applications.[21,22]

We have already investigated Möbius Zn(II) hexaphyrin complexes in which multiple sources of chirality can operate to favor *P* or *M* twists: *information relay* phenomena occurred when two sources of chirality were embedded in a covalent capping unit (Figure 1b, left);[18b] *match/mismatch* phenomena were observed when two exogenous chiral ligands were bound to zinc (Figure 1b, right).[18c,d] In a different strategy, switching the *P*/*M* configuration of a Möbius Zn(II) hexaphyrin complex functionalized with a chiral coordinating arm was successfully achieved (Figure 1c, left).[18e] The concomitant coordination and release of an exogenous achiral effector to zinc is a key step to control the position and orientation of the chiral arm relative to the ring, hence the tunable chirality induction.

The next degree of sophistication has consisted in the design of a system involving two different Möbius hexaphyrins in which multiple chirality induction phenomena at the level of the twisted π-systems could be finely manipulated. The emergence of complex chemical behaviors from mixtures of interacting molecules is a general feature of natural systems, which has inspired a growing area of research called *systems chemistry*.[8a,23] To the best of our knowledge, studying mixtures of different dynamic Möbius π-systems has not been reported so far. Understanding complex behaviors from Möbius-type transformation networks would provide an interesting starting point for new developments in systems chemistry, responsive materials or switchable catalytic machineries.[8b]

To do so, we envisioned the preparation of new hexaphyrin ligands according to a reversed engineering (Figure 1c, right). More precisely, we have introduced a single chiral amino arm to complement our previous system with a carboxylic acid one,[18e] expecting that both Möbius rings mixed together could be addressed by coordination of specific exogenous achiral ligands. Herein, we investigate chirality induction processes driven by zinc complexation from mixtures of such dynamic Möbius ligands, aiming at the achievement of chiroptically active Möbius-type stereoselective transformation networks.

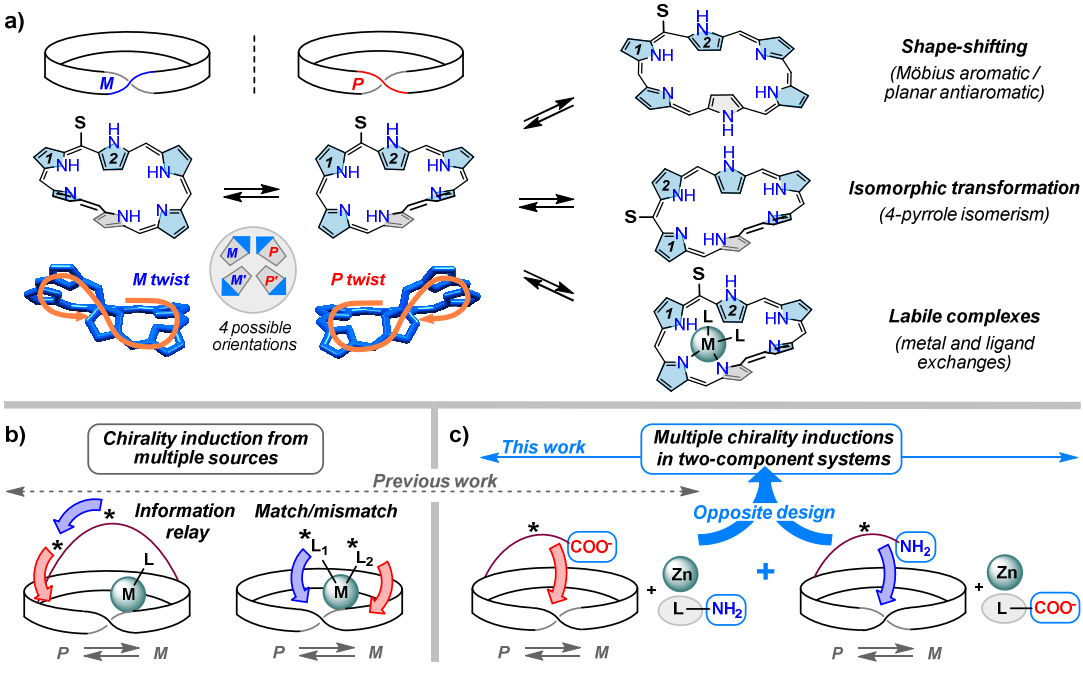

Figure 1. a) Left: the two enantiomers of a Möbius band (singly twisted) and equilibrium between those of a regular Möbius [28]hexaphyrin; right: common dynamic processes encountered with this scaffold ("S" stands for a *meso* substituent). b) Chirality induction with labile Zn(II) complexes of Möbius [28]hexaphyrins, tuned by the influence of two chiral sources. c) Investigated strategy based on a reversed design: Möbius [28]hexaphyrins functionalized with a chiral carboxylato/amino coordinating arm.

Results and discussion

Synthesis and conformational study

The recently described [26]hexaphyrin **1** (Scheme 1) consists of a dynamic mixture of two isomers with the 2-nitrophenyl *meso* substituent located either on a short or a long side of the rectangle.[18e] Upon reduction of the nitro group by H_2/Pd(C), the grafting of amino arms with different steric encumbrance and flexibility was achieved in moderate yields by reaction with commercially available N-Boc protected amino acids, which were beforehand activated as mixed anhydrides (Scheme 1, inset). The targeted compounds **6a-c**, ***(1S3R)*-8** and ***(S)*-10** were obtained in good yields upon subsequent Boc deprotection with trifluoroacetic acid (TFA). Compounds **5** to **10** were isolated in their reduced [28]π state, as inferred from HRMS analysis, and have the characteristic blue color of Möbius aromatic hexaphyrins. Their UV-vis absorption spectra exhibit a sharp and intense Soret-like band at ~595 nm as well as weak Q-like bands in the NIR region (up to ~1000 nm) (Figure S1).

^{1}H and ^{19}F NMR spectra of **5-10** in $CDCl_3$ are broadened and very sensitive to temperature variations (223 – 330 K, SI), in accordance with the usual conformational mobility of Möbius regular [28]hexaphyrins. Neither the precise *meso* position of the arm and its *up*/*down* orientation relative to the ring, nor chirality induction at the level of the twisted π-system for compounds equipped with a chiral arm, could be determined. However, comparison of the different VT NMR patterns complemented with 2D ROESY spectra recorded at 330 K gave us insights in the dynamic features of these compounds (see details in the SI):[24]

(i) For most of the compounds, a single dissymmetric pattern was observed at 330 K with differentiated *outer*, *inner* and *twisted* β-pyrrolic protons, meaning that, although dynamic and thus having averaged NMR patterns (*vide infra*), they adopt a preferential Möbius conformation with a localized twist and a single *meso* position of the arm;

(ii) At 330 K, selective exchange correlations between *outer* β-pyrrolic protons revealed a degenerate equilibrium (slow process on the NMR time scale) according to a four-pyrrole isomerism ("isomorphic transformation", Figure 1a). This further indicates that the arm is localized on a residual long side of the Möbius scaffold;

(iii) At lower temperatures, either one or two splitting/broadening processes were observed, respectively with compounds having an achiral and a chiral arm. One process is in the range 330 – 280 K, for chiral arms, and the second process is in the range 280 – 223 K for both chiral and achiral arms. These are in agreement with a rotation of the *meso*-phenyl unit bearing the arm which becomes fast on the NMR time scale at high temperatures (atropisomerism), and with an interconversion between different twisted conformations (*i.e. P,P',M,M'*, Figure 1a) which tends to be frozen at low temperatures.

This conformational flexibility is of great interest as it enables the formation of a virtual dynamic library of ligands, in which the coordinating arm is prompt to explore the Möbius ring environment and respond to changes in the experimental conditions.

Scheme 1. Synthesis of [28]hexaphyrins 6a-c, (*1S3R*)-8 and (*S*)-10 bearing a single amino arm.[a]

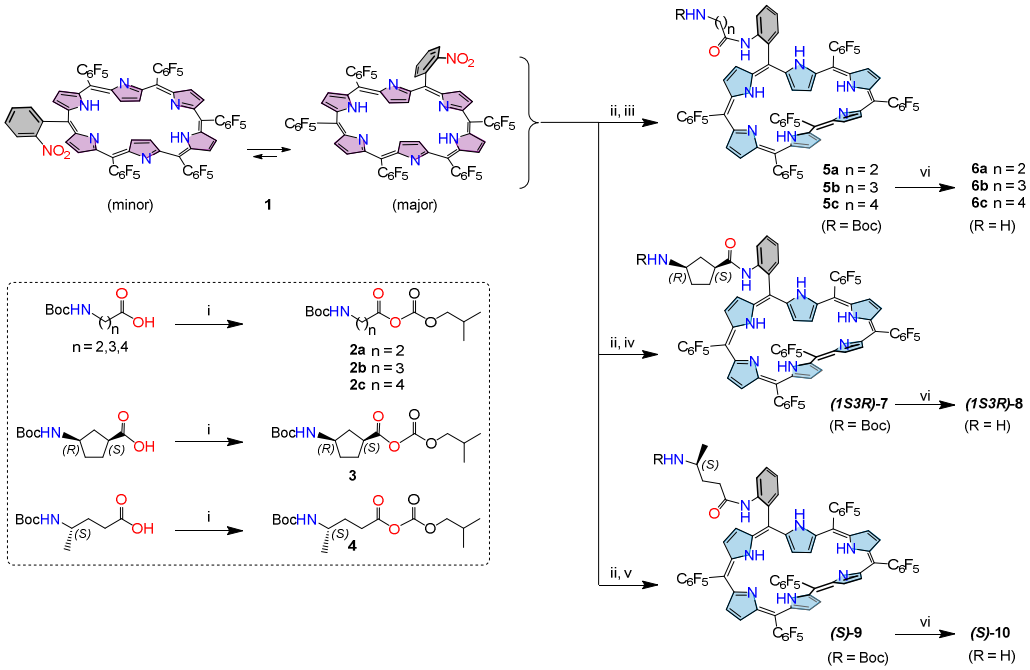

[a] Dynamic compounds; *P* twist arbitrarily displayed for clarity. Conditions: (i) isobutylchloroformiate, N-methylpiperidine, THF, RT; (ii) H_2 (80 bar), Pd(0)/C cat., AcOEt, RT, 15 h; (iii) **2a-c**, TEA, THF, RT, 1 h (**5a**, 30 %; **5b**, 70 %; **5c**, 21 %); (iv) **3**, TEA, THF, RT, 1 h (***(1S3R)*-7**, 55 %); (v) **4**, TEA, THF, RT, 1 h (***(S)*-9**, 72 %); (vi) TFA, DCM then NaOH (**6a**, 85 %; **6b**, quant.; **6c**, quant.; ***(1S3R)*-8**, quant.; ***(S)*-10**, 82 %).

For chiral compounds **7** to **10**, ECD analysis revealed Cotton effects of moderate intensity in the Soret wavelength region (Figure 2, $\Delta\varepsilon_{616}$ up to 140 $M^{-1}cm^{-1}$). Interestingly, compounds ***(1S3R)*-7** and ***(1S3R)*-8** exhibit ECD spectra that are almost mirror images (Figure 2b), meaning that simple deprotection of the amine function leads to reversed chirality induction at the level of the Möbius π system. In contrast, both compounds ***(S)*-9** and ***(S)*-10** exhibit a positive Cotton effect, but that of the latter is more than twice weaker (Figure 2a). Moreover, whereas the ECD intensity of ***(S)*-10** was unaffected by addition of MeOH, that of ***(S)*-9** was strongly weakened (Figure S2). It suggests that the NHBoc group interacts by H-bonding with a pyrrole unit. Taken together, these observations indicate highly tunable chirality induction processes (not quantifiable at this stage) owing to various interaction modes of the chiral arm with the dynamic hexaphyrin scaffold, evidencing an adaptive Möbius π system.

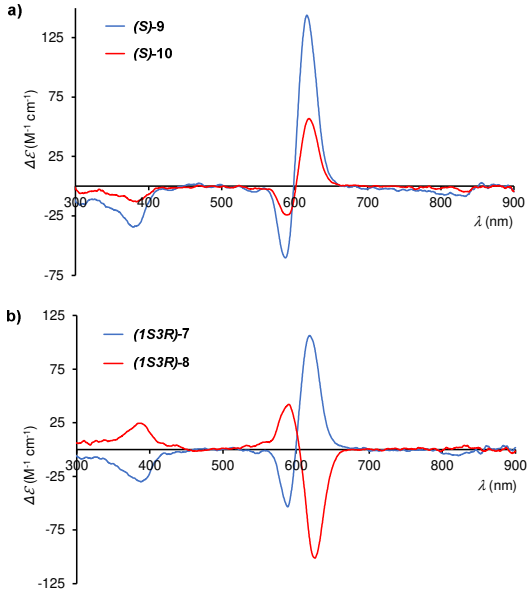

Figure 2. ECD spectra ($CHCl_3$) of compounds ***(1S3R)*-7**, ***(1S3R)*-8**, ***(S)*-9** and ***(S)*-10**.

Coordination of Zn(II) and chirality induction

In the next step, Zn(II) complexation by the newly formed Möbius [28]hexaphyrins was investigated by NMR spectroscopy in a 9:1 $CDCl_3/CD_3OD$ mixture, in the presence of diisopropylethylamine (DIPEA). For all compounds **5**-**10**, addition of 1 equiv. of $Zn(OTf)_2$ led to weak complexation if any, only minor sets of signals being observed (Figures S16-S18). This situation was drastically improved by adding ~5 equivalents of tetrabutylammonium acetate (TBAOAc), but only for compounds having a deprotected amino arm. For instance, multiple patterns were observed in the case of Boc protected **5b** instead of a single one for its deprotected counterpart **6b** (Figure 3a,b). The complicated pattern obtained with **5b** likely corresponds to a mixture of several 'ZnOAc' Möbius aromatic complexes with both a solvent molecule and AcO^- bound to zinc (**5b^M.Zn$_{OAc}$**, Scheme 2).[18c] With **6b**, an initial ~1:0.8 mixture of two 'ZnOAc' complexes was formed corresponding to the Möbius aromatic complex **6b^M.Zn$_{OAc}$** and the Hückel (rectangular) antiaromatic one **6b^H.Zn$_{OAc}$** (Scheme 2, Figure S17). This mixture gradually converts to the Möbius complex quasi-quantitatively after several hours at RT. Complexes **6b^M.Zn$_{OAc}$** and **6b^H.Zn$_{OAc}$** exhibit characteristic shielding/deshielding effects resulting from diatropic and paratropic ring currents, respectively. For instance, the methyl group of the ZnOAc moiety is shielded by 2.83 ppm for **6b^M.Zn$_{OAc}$** and deshielded by 4.29 ppm for **6b^H.Zn$_{OAc}$**, in agreement with an *inward* orientation of the acetato ligand for both complexes. The β-pyrrolic protons of **6b^M.Zn$_{OAc}$** are split into three areas, the *inner* ones at -2.61 and -1.95 ppm, the *twisted* ones at 5.06 and 5.53 ppm and the eight *outer* ones ranging from 6.80 to 8.15 ppm (Figure 3b). For **6b^H.Zn$_{OAc}$**, they are split into two areas, in the range 15.40-16.00 ppm for the four *inner* ones and roughly ranging from 3 to 5 ppm for the eight *outer* ones (Figure S17). Owing to NOE correlations (Scheme 2, Figure S25), the *meso* position of the amino arm of **6b^M.Zn$_{OAc}$** was assigned to a residual short side adjacent to the dipyrrin binding site, as drawn in Scheme 2. This location is fully consistent with an intramolecular *outward* coordination of the amino group to Zn,[25] explaining the greater selectivity *vs* **5b**. For **6b^H.Zn$_{OAc}$**, the dissymmetric pattern matches with a long side *meso* position of the arm, coordinated *outward* to zinc (Scheme 2).[26]

Scheme 2. Zn(II) complexation behavior of 5b, 6b and *(S)*-10.[a]

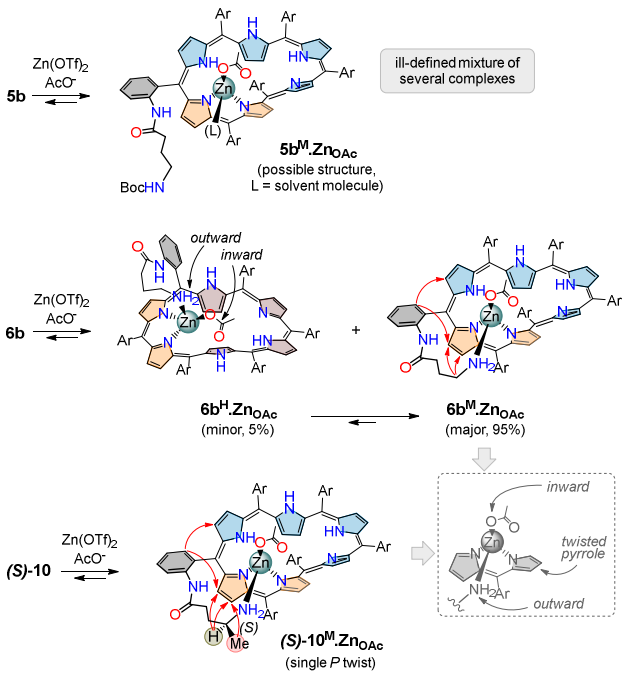

[a] Red arrows correspond to NOE correlations. Ar = C_6F_5.

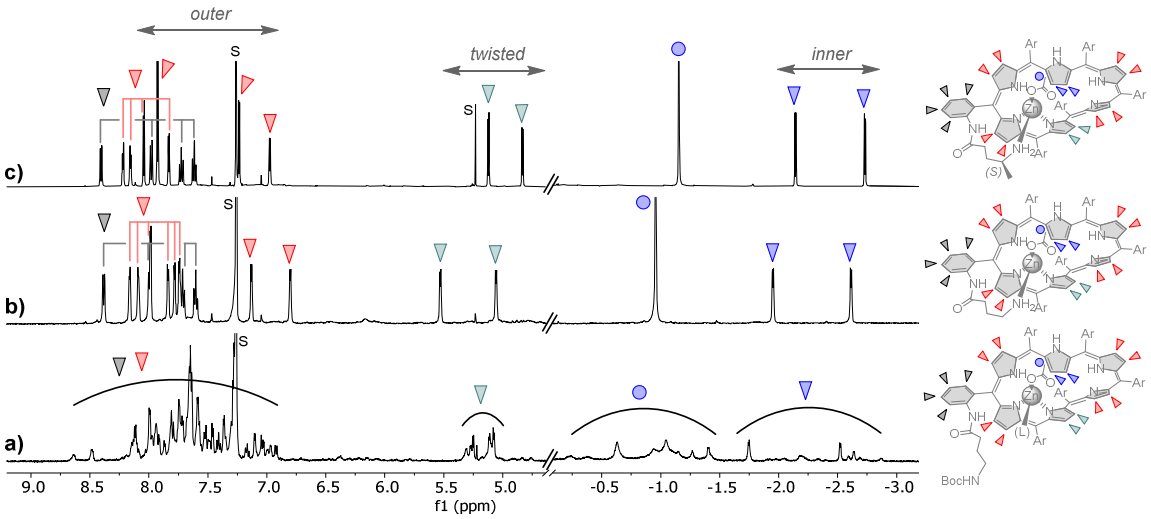

Figure 3. ^{1}H NMR spectra of complexes (a) **5b^M.Zn$_{OAc}$** (mixture), (b) **6b^M.Zn$_{OAc}$** and (c) ***(S)*-10^M.Zn$_{OAc}$** ($CDCl_3/CD_3OD$ 9:1, 300K; selected areas). S = solvent.

The two other ligands **6a** and **6c** with respectively a shorter and a longer amino arm led to much less selective complexation processes. While negligible amounts of antiaromatic rectangular 'ZnOAc' complexes were observed, mixtures of respectively two and three Möbius 'ZnOAc' complexes were formed instead of a single one for **6b** (**6a^M.Zn$_{OAc}$** and **6c^M.Zn$_{OAc}$**, see details in the SI). It is likely that the coordination of the amino function to zinc is much less effective and/or does not act as a driving force. In addition, competitive ^{1}H NMR experiments evidenced a higher affinity of 'ZnOAc' for **6b** compared to **6a** and **6c** (Figure S19). All these observations indicate an optimum 'C3' length of the arm, affording highest selectivity and affinity due to an efficient intramolecular zinc coordination.

In the next step, we focused on hexaphyrins ***(1S3R)*-8** and ***(S)*-10**, both with a chiral amino arm derived from the C3 chain. For ***(1S3R)*-8**, using $Zn(OTf)_2$ and TBAOAc, we were not able to find experimental conditions leading to a selective complexation. In the best situation, ^{1}H NMR analysis evidenced a highly complex mixture, among which a minor rectangular antiaromatic species and three major Möbius aromatic ones were identified, all of them exhibiting an *inward* ZnOAc moiety (see details in the SI). The corresponding ECD spectrum revealed very weak chiroptical activity, in agreement with a lack of *P*/*M* stereoselectivity (Figure S20). In strong contrast, in presence of $Zn(OTf)_2$ and TBAOAc, hexaphyrin ***(S)*-10** led to an initial mixture of only two compounds with antiaromatic and aromatic signatures, which converted quantitatively to the aromatic one in a couple of hours (Figure 3c and S18). The obtained Möbius zinc complex is very similar to **6b^M.Zn$_{OAc}$**, and corresponds to ***(S)*-10^M.Zn$_{OAc}$** with a single *P* twist (Scheme 2). Indeed, while NOE correlations evidenced a coordinating arm located on a residual short side and constrained above an *outer* pyrrole bound to zinc (Scheme 2, Figure S37), the ECD spectrum revealed an intense positive Cotton effect in the Soret band region ($\Delta\varepsilon_{627}$ up to 634 $M^{-1}cm^{-1}$, Figure 4), indicating a right-handed helicity of the π-system. Such a quantitative complexation corresponds not only to a high '*meso-position*' selectivity, but also to a rarely achieved *P*/*M* stereoselectivity with a *d.e.* value much greater than 95 %. The ECD spectrum of ***(S)*-10^M.Zn$_{OAc}$** matches that of our previously described system featuring an opposite engineering (***(RR)*-11.Zn^{NH_2Bu}**, Figure 4 and Scheme 3),[18e] although slightly weaker.

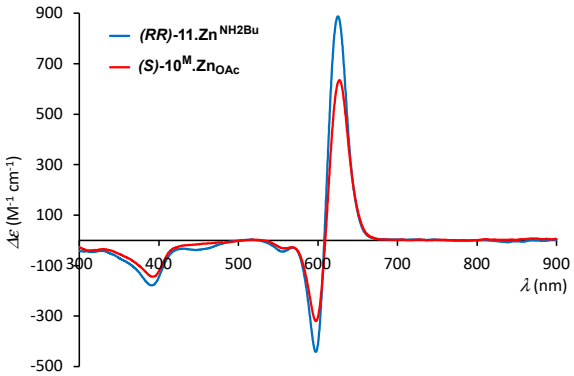

Figure 4. ECD spectra of ***(S)*-10^M.Zn$_{OAc}$** and of the previously described complex ***(RR)*-11.Zn^{NH_2Bu}** ($CHCl_3/CH_3OH$ 9:1).[18e]

This stereoselectivity was rationalized from the modeled structure of ***(S)*-10^M.Zn$_{OAc}$** (Figure 5). The zinc coordination of the amino arm induces a conformational restriction placing the "H" and "Me" substituents of the asymmetric carbon in well-defined positions. Whereas the bulkier "Me" moiety is oriented laterally without noticeable interaction with the surrounding fluorine atoms (Figure 5b,c), the smaller "H" substituent is oriented towards the centroid of the *outer* pyrrole coordinated to zinc, at short distance (*ca.* 2.5 Å, Figure 5b,c). It is assumed that the opposite configuration of the asymmetric carbon within the same *P* twist environment would generate steric repulsion since the

"Me" moiety would point towards the *outer* pyrrole bound to zinc. Looking back at ***(1S3R)*-8**, it is likely that the bulkier cyclopentyl unit induces a steric clash with the hexaphyrin skeleton upon coordination to zinc, with both *P* and *M* stereoisomers.

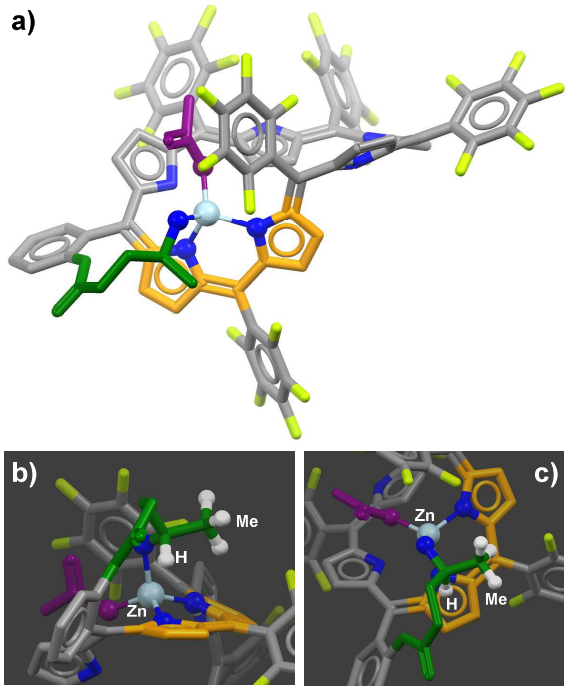

Figure 5. Energy minimized structure of ***(S)*-10^{M}.Zn$_{OAc}$**, highlighting the orientations of the "H" and "Me" substituents of the asymmetric carbon of the coordinating arm: (a) general view; (b) side view from the coordinating arm; (c) top view of the coordination site (ball and stick representation; molecular mechanics performed with UFF force field parameters in Avogadro; H atoms removed for clarity except those labelled in b and c; dipyrin binding site: orange; zinc: light blue; coordinating arm: green; acetato ligand: purple).

Formation of two-component systems

Having in hand two complementary Möbius hexaphyrin ligands, both leading to nearly quantitative Möbius twist stereoselectivity (***(S)*-10^{M}.Zn$_{OAc}$** and ***(RR)*-11.Zn^{NH2Bu}**), we then investigated their general zinc complexation behavior once mixed together. It is worth reminding that the complexation of zinc by compound ***(RR)*-11**, a Möbius [28]hexaphyrin functionalized with a chiral coordinating arm ending a carboxylate function, was recently investigated by our group (Figure 1c, Scheme 3).[18e] Two well-defined complexes with opposite twist configuration were formed depending on the nature of an exogenous achiral ligand (AcO^-/$BuNH_2$), influencing the position of the arm and the ensuing transfer of chirality.

Thus, a two-component mixture was generated by mixing [28]hexaphyrins **6b** (/***(S)*-10**) and ***(RR)*-11** in 1:1 ratio at millimolar concentration in a $CDCl_3/CD_3OD$ 9:1 solution, after what a slight excess of $Zn(OTf)_2$ was added. The corresponding ^1H NMR spectrum revealed a complex pattern with multiple broad and ill-defined signals, but different from the sum of the patterns of the separated hexaphyrins in the same conditions (Figure 6b,g and S40). At first glance, this indicates that the two hexaphyrins interact together forming coordination assemblies. Several observations suggest intermolecular zinc coordination of the amino and carboxylato arms, leading to a complex mixture of heterodimers (see details in the SI).

Scheme 3. Structures and interconversion of previously described zinc complexes from Möbius [28]hexaphyrin *(RR)*-11, used in this study.[a,18e]

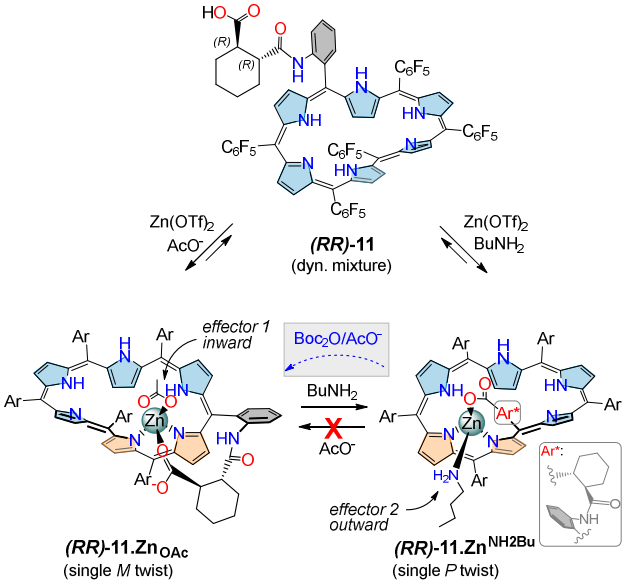

[a] Ar = C_6F_5.

This situation was strongly modified by the subsequent addition of achiral effectors (Scheme 4).[27] We observed that addition of only AcO^- contributed to the formation of both **6b^{M}.Zn$_{OAc}$** (/***(S)*-10^{M}.Zn$_{OAc}$**) and ***(RR)*-11.Zn$_{OAc}$** (Figure 6c,h) whereas addition of only $BuNH_2$ led to the formation of ***(RR)*-11.Zn^{NH2Bu}** (Figure 6d,i). Remarkably, the addition of both $BuNH_2$ and TBAOAc (~5 equiv. each) afforded, independently of their order of introduction, a 1:1 mixture of the Möbius complexes **6b^{M}.Zn$_{OAc}$** (/***(S)*-10^{M}.Zn$_{OAc}$**) and ***(RR)*-11.Zn^{NH2Bu}** with high selectivity (Figure 6e,j; Scheme 4).[28] Such a behavior is related to a social self-sorting phenomenon in the sense that an hexaphyrin with a carboxylate (respectively an amine) arm binds selectively an exogenous ligand with an amine (respectively a carboxylate) function.[29] Such a high fidelity recognition process involving five different species (two hexaphyrins, two exogenous ligands, one metal ion) has been scarcely described in the field of expanded porphyrins,[18a] and is unprecedented with Möbius molecular rings. It is even more important to note that chirality inductions proceed in parallel manner with the same high efficiency whether the hexaphyrin complexes are alone or mixed, provided that suitable achiral effectors have been added.

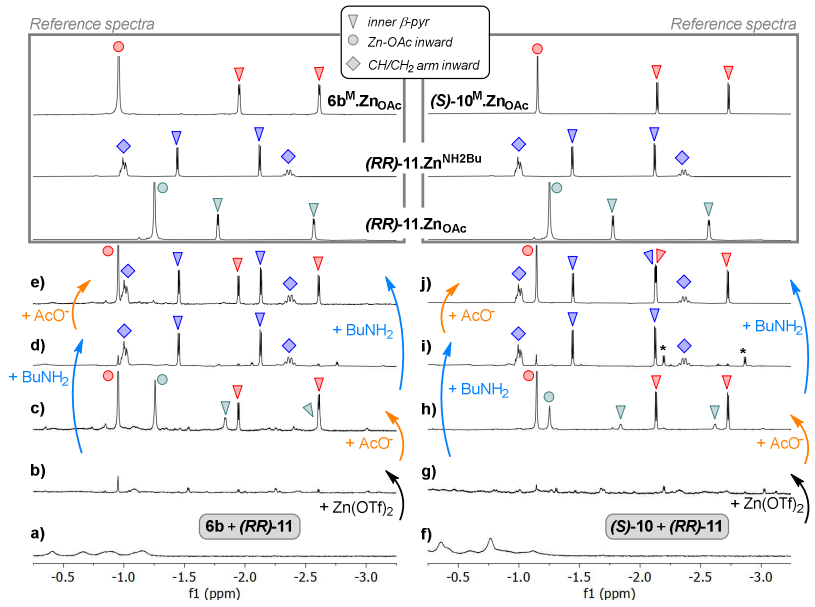

Figure 6. ^{1}H NMR spectra (high-field region) corresponding to the complexation of zinc by two-component mixtures of **6b**/***(RR)*-11** (a-e) and ***(S)*-10**/***(RR)*-11** (f-j) ($CDCl_3/CD_3OD$ 9:1, 300 K, 500 MHz). * : unidentified species.

Scheme 4. Zinc complexation by a 1:1 mixture of *(RR)*-11 with either 6b or *(S)*-10, combined to a single-component chemical switch.[a]

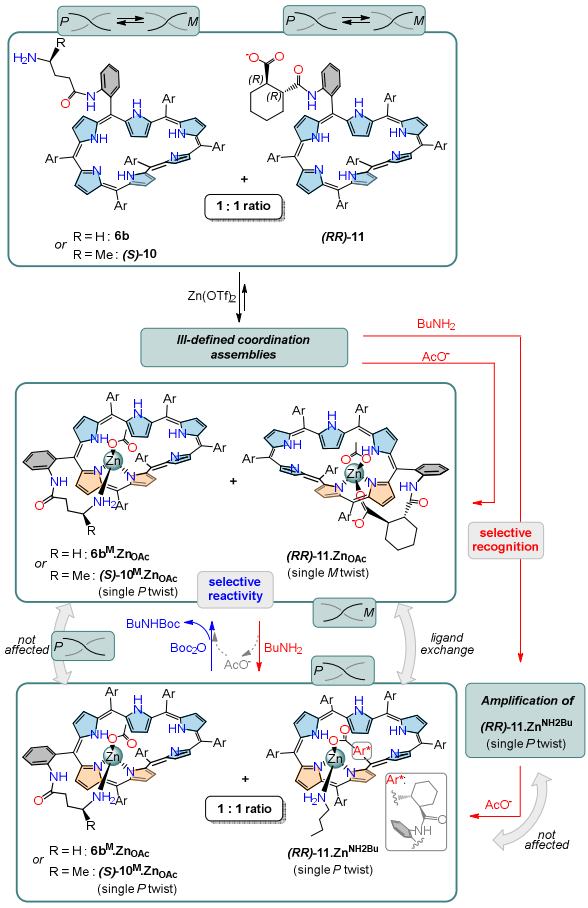

[a] Ar = C_6F_5.

Zinc complexation has therefore a deep influence on the chiroptical activity of the ensembles. Whereas 1:1 mixtures of ***(RR)*-11** with either **6b** or ***(S)*-10** led to almost flat ECD spectra (Figure 7a,c), subsequent addition of $Zn(OTf)_2$, TBAOAc and $BuNH_2$ led to a drastic increase of the signatures with intense positive Cotton effects at the level of the Soret band (Figure 7b,d). The global chiroptical activity corresponds to the sum of the contributions of each components, *i.e.* **$6b^M.Zn_{OAc}$/*(RR)*-11.Zn^{NH_2Bu}** (racemic/*P* twist) and ***(S)*-$10^M.Zn_{OAc}$/*(RR)*-11.Zn^{NH_2Bu}** (*P* twist/*P* twist), and is logically raised by a factor ~1.7 when both Möbius complexes exhibit similar chirality inductions.[30]

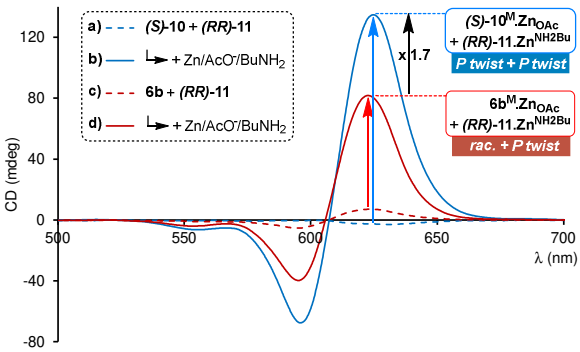

Figure 7. Comparison of ECD spectra of 1:1 mixtures of two hexaphyrins (***(RR)*-11** with either **6b** or ***(S)*-10**) before (dashed lines) and after (plain lines) addition of $Zn(OTf)_2$, TBAOAc and $BuNH_2$ ($CHCl_3$/MeOH 9:1; all spectra were recorded at the same concentration).

This two-component approach thus offers the possibility for parallel chirality induction phenomena, which corresponds to a different behavior as compared to our recent findings involving several sources of chirality (Figure 1b).[18b,c] These results encouraged us for the further (stereo)selective transformation of the mixture.

Modulation of two-component systems

In the next step, we have attempted to address selectively one of the two components of the above described mixtures. For that, we used a chemical switching process recently reported between amino and acetato zinc complexes of ***(RR)*-11**, whose working principle lies on the successive additions of Boc_2O and $BuNH_2$ (respectively forward and backward processes), in the presence of AcO^- (Scheme 3).[18d,e]

We first checked that complex ***(S)*-10^{M}.Zn$_{OAc}$** with an amino arm was compatible with such Boc protection reaction. For that, the free base hexaphyrin ***(S)*-10** and the complex ***(S)*-10^{M}.Zn$_{OAc}$** were treated with 7 equiv. excess of Boc_2O and heated at 50 °C. While ***(S)*-10** was fully converted to its Boc derivative within 45 min, any noticeable modification of the ^{1}H NMR spectrum of ***(S)*-10^{M}.Zn$_{OAc}$** was not observed, even after prolonged heating (Figure S44). This comparison evidences an efficient protection of the amino function of the arm by its intramolecular coordination to zinc.[31]

We then formed a 1:1 mixture of ***(S)*-10^{M}.Zn$_{OAc}$** and ***(RR)*-11.Zn^{NH_2Bu}** and added a slight excess of Boc_2O compared to the total amount of $BuNH_2$. After heating 60 min at 50 °C leading to the Boc protection of $BuNH_2$, we observed that ~ 95 % of ***(RR)*-11.Zn^{NH_2Bu}** was consumed and converted with ~ 60 % efficiency to ***(RR)*-11.Zn$_{OAc}$** (Figure 8a,b, blue to green triangles; Scheme 4). In this step, the complementary complex ***(S)*-10^{M}.Zn$_{OAc}$** was not affected (Figure 8b, red triangles). The backward process was realized by simple addition of $BuNH_2$, leading quasi-quantitatively to the initial 1:1 two-component mixture in ~10 min (Figure 8c). This compartmentalized switching process, successfully repeated 5 times (Figure 8a-j), proceeds with an efficiency comparable to that of the single-component version.[18e]

ECD monitoring evidenced switching between two chiroptical states with large amplitude variation (Figure 9a, bottom). In the initial state, the two complexes ***(S)*-10^{M}.Zn$_{OAc}$** and ***(RR)*-11.Zn^{NH_2Bu}** exhibit a positive Cotton effect (*P* twist, Figure 4), while in the second state (*i.e.* upon addition of Boc_2O), the formed complex ***(RR)*-11.Zn$_{OAc}$** exhibits a weaker Cotton effect of opposite sign.[18e] Therefore, the chiroptical activity of ***(S)*-10^{M}.Zn$_{OAc}$**, initially boosted by the presence of ***(RR)*-11.Zn^{NH_2Bu}**, is successively restored and amplified upon additions of Boc_2O and $BuNH_2$ (Figure 9a, top).

Using complex ***(SS)*-11.Zn^{NH_2Bu}**, having opposite chiroptical activity to the *(RR)* isomer (negative Cotton effect, *M* twist), in the two-component mixture with ***(S)*-10^{M}.Zn$_{OAc}$**, the opposite behavior was observed (Figure 9b). The chiroptical activity of ***(S)*-10^{M}.Zn$_{OAc}$**, initially masked by the presence of ***(SS)*-11.Zn^{NH_2Bu}**, is successively restored and masked again upon additions of Boc_2O and $BuNH_2$. Complex ***(SS)*-11.Zn^{NH_2Bu}** was also combined with **6b.Zn$_{OAc}$** (racemic, deprived of chiroptical activity) and submitted to the Boc_2O/$BuNH_2$ switching procedure. The result is comparable to the previous situation, but shifted to the negative values (Figure 9c *vs* b).

In summary, by changing the nature and twist configuration of only one of the two complexes, at initial state or by switching, this approach enables a 'two-channel' tuning of the chiroptical properties of the ensemble. Overall, it results from a fine control of two *in fine* independent (parallel) chirality induction processes in a complex mixture under thermodynamic control, giving rise to a chiroptically active stereoselective transformation network.

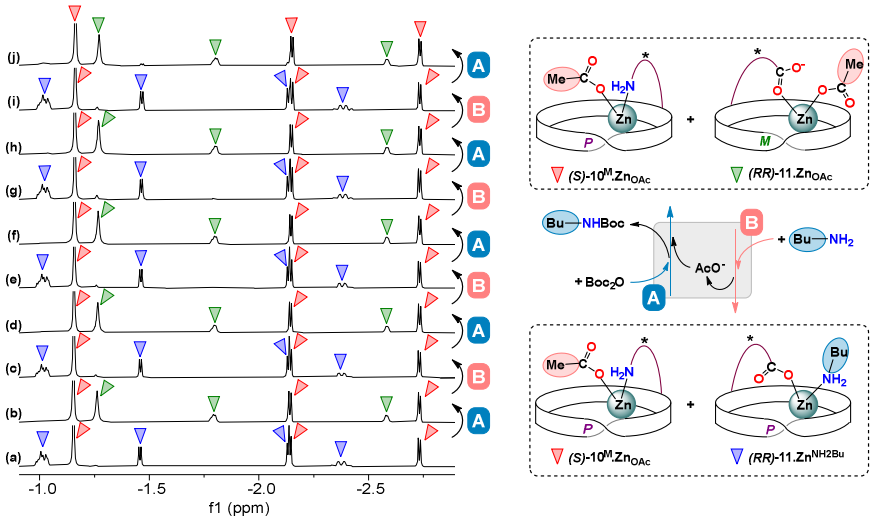

Figure 8. ^{1}H NMR spectra (high-field region) corresponding to the chemical switching between a 1:1 mixture of ***(S)*-10^{M}.Zn$_{OAc}$** and ***(RR)*-11.Zn^{NH_2Bu}**, and a mixture of ***(S)*-10^{M}.Zn$_{OAc}$** and ***(RR)*-11.Zn$_{OAc}$** ($CDCl_3$/CD_3OD 9:1, 300 K, 500 MHz). Forward process ("A"): addition of Boc_2O, 50 °C, 60 min; backward process ("B"): addition of $BuNH_2$, RT, 10 min.

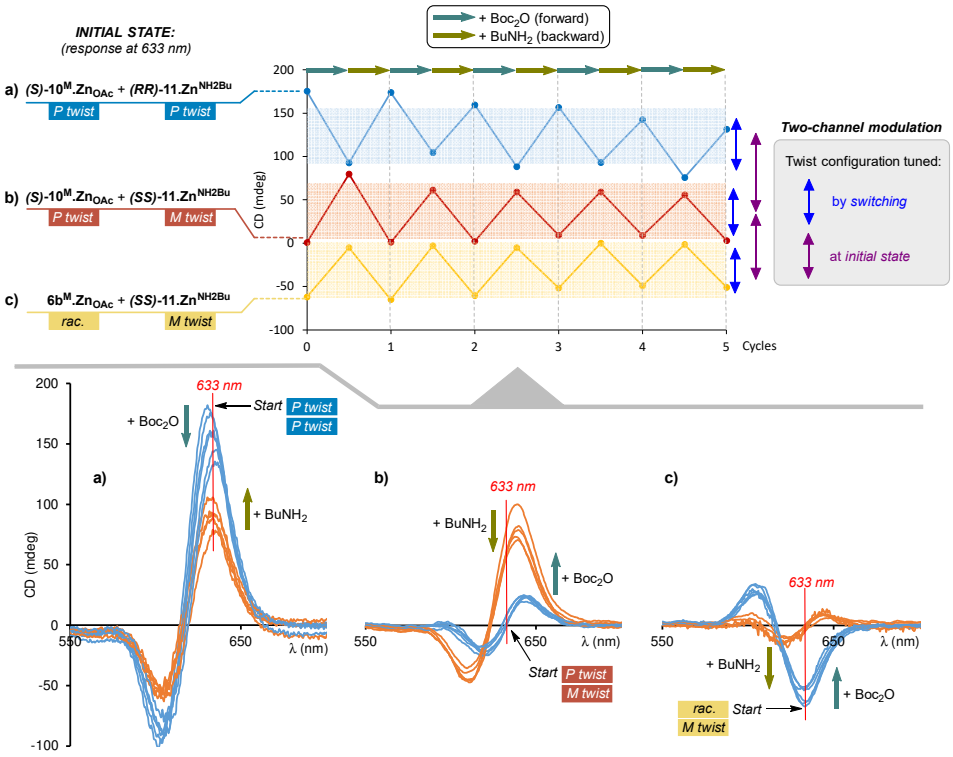

Figure 9. ECD monitoring of the $Boc_2O/BuNH_2$ chemical switching starting from different 1:1 mixtures: a) ***(S)*-10^{M}.Zn$_{OAc}$** and ***(RR)*-11.Zn^{NH2Bu}**; b) ***(S)*-10^{M}.Zn$_{OAc}$** and ***(SS)*-11.Zn^{NH2Bu}**; c) **6b^{M}.Zn$_{OAc}$** and ***(SS)*-11.Zn^{NH2Bu}** (bottom: Soret band region; top: values at 633 nm. Spectra/values are uncorrected with respect to concentration variations).

Conclusion

The grafting of various coordinating arms ending an amino function to the dynamic Möbius [28]hexaphyrin scaffold has been successfully achieved. The further complexation of zinc was fruitful, leading to the following main advances:

Reversed engineering. With a chiral amino arm, an achiral effector such as AcO^- controls chirality induction to the twisted π-system leading to a rarely achieved single twist configuration (*e.d.* > 95 %). As a result, the zinc complex exhibits strong chiroptical activity with intense Cotton effect at ~ 630 nm.

Social self-sorting and parallel stereoselections. Mixing two complementary Möbius [28]hexaphyrins, *i.e.* featuring chiral arms with either amino or carboxylato coordinating functions, led very selectively to 1:1 mixtures of zinc complexes provided their corresponding achiral effectors have been added (respectively $AcO^-/BuNH_2$). Chirality inductions are not affected with respect to the separated complexes and are still impressive, opening the way to well defined multiple chiroptical switches.

Compartmentalized transformations. From these two-component mixtures, it was possible to address selectively and reversibly one of the two Möbius complexes by reacting the $BuNH_2$ effector with Boc_2O. Therefore, the chiroptical activity of only one part of the mixture can be switched, enabling *in fine* a two-channel modulation of the global chiroptical property of the ensemble. In this complex dynamic system, selective recognition and selective reactivity are key processes responsible for controlled chirality induction phenomena.

The [28]hexaphyrin scaffold appears one of the most powerful source of Möbius-type platforms. It enables multiple dynamic chirality inductions of interest to create novel chiral adaptive systems. Aiming at clever networks, we are actively working on multi-component Möbius systems in which each of the components could be manipulated independently *via* orthogonal and non-invasive stimuli.

ASSOCIATED CONTENT

Supporting Information. Full experimental details and spectral data (PDF). This material is available free of charge via the Internet at http://pubs.acs.org.

AUTHOR INFORMATION

Corresponding Author

* stephane.legac@univ-rennes.fr.

Notes

The authors declare no competing financial interest.

ACKNOWLEDGMENT

We are grateful to the Ministère de l'Enseignement Supérieur et de la Recherche for a doctoral grant allocated to TN.

REFERENCES

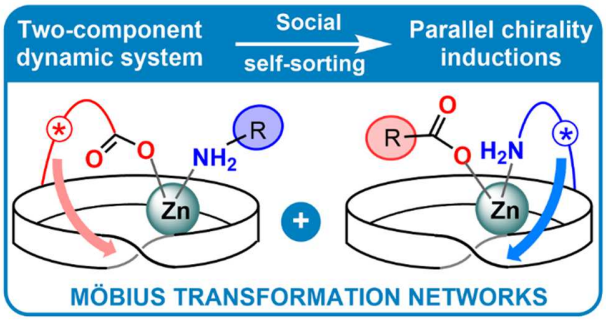

[1] Selected reviews covering the field of expanded porphyrins: (a) Sessler, J. L.; Seidel, D. Synthetic Expanded Porphyrin Chemistry. *Angew. Chem., Int. Ed.* **2003**, *42*, 5134-5175. (b) Yoon, Z. S.; Osuka, A.; Kim, D. Möbius Aromaticity and Antiaromaticity in Expanded Porphyrins. *Nat. Chem.* **2009**, *1*, 113-122. (c) Shin, J.-Y.; Kim, K. S.; Yoon, M.-C.; Lim, J. M.; Yoon, Z. S.; Osuka, A.; Kim, D. Aromaticity and Photophysical Properties of Various Topology-Controlled Expanded Porphyrins. *Chem. Soc. Rev.* **2010**, *39*, 2751-2767. (d) Stępień, M.; Sprutta, N.; Latos-Grażyński, L. Figure Eights, Möbius Bands, and More: Conformation and Aromaticity of Porphyrinoids. *Angew. Chem., Int. Ed.* **2011**, *50*, 4288-4340. (e) Saito, S.; Osuka, A. Expanded Porphyrins: Intriguing Structures, Electronic Properties, and Reactivities. *Angew. Chem., Int. Ed.* **2011**, *50*, 4342-4373. (f) Osuka, A.; Saito, S. Expanded Porphyrins and Aromaticity. *Chem. Commun.* **2011**, *47*, 4330-4339. (g) Roznyatovskiy, V. V.; Leeb, C.-H.; Sessler, J. L. π-Extended Isomeric and Expanded Porphyrins. *Chem. Soc. Rev.* **2013**, *42*, 1921-1933. (h) Tanaka, T.; Osuka, A. Chemistry of *meso*-Aryl-Substituted Expanded Porphyrins: Aromaticity and Molecular Twist. *Chem. Rev.* **2017**, *117*, 2584-2640. (i) Mo Sung, Y.; Oh, J.; Cha, W.-Y.; Kim, W.; Min Lim, J.; Yoon, M.-C.; Kim, D. Control and Switching of Aromaticity in Various All-Aza-Expanded Porphyrins: Spectroscopic and Theoretical Analyses. *Chem. Rev.* **2017**, *117*, 2257-2312. (j) Szyszko, B.; Białek, M. J.; Pacholska-Dudziak, E.; Latos-Grażyński, L. Flexible Porphyrinoids. *Chem. Rev.* **2017**, *117*, 2839-2909.

[2] Confined spaces have recently been tuned thanks to hexaphyrin rearrangement in capped molecular systems: (a) Le Gac, S.; Boitrel, B.; Sollogoub, M.; Ménand, M. Protonated Hexaphyrin-Cyclodextrin Hybrids: Molecular Recognition Tuned by a Kinetic-to-Thermodynamic Topological Adaptation. *Chem. Commun.* **2016**, *52*, 9347-9350. (b) Ménand, M.; Sollogoub, M.; Boitrel, B.; Le Gac, S. Cyclodextrin-Sandwiched Hexaphyrin Hybrids. Side-to-Side Cavity Coupling Switched by a Temperature and Redox Responsive Central Device. *Chem. Eur. J.* **2018**, *24*, 5804-5812. (c) Le Gac, S.; Caytan, E.; Dorcet, V.; Boitrel, B. Acid-Base Controlled Multiple Conformation and Aromaticity Switches in Tren-Capped Hexaphyrins. *Org. Biomol. Chem.* **2019**, *17*, 3718-3722.

[3] Kovbasyuk, L.; Krämer, R. Allosteric Supramolecular Receptors and Catalysts. *Chem. Rev.* **2004**, *104*, 3161-3188.

[4] Molecular Switches. Browne, W. R.; Feringa, B. L., Eds, Wiley-VCH, Weinheim, 2011, vol. I, II.

[5] For shape-shifting ligands and coordination cages based on the bullvalene moieties, see: (a) Bismillah, A. N.; Chapin, B. M.; Husseina, B. A.; McGonigal, P. R. Shapeshifting molecules: the story so far and the shape of things to come. *Chem. Sci.* **2020**, *11*, 324-332. (b) Birvé, A. P.; Patel, H. D.; Price, J. R.; Bloch, W. M.; Fallon, T. Guest-Dependent Isomer Convergence of a Permanently Fluxional Coordination Cage. *Angew. Chem. Int. Ed.* **2022**, *61*, e202115468.

[6] For a rare example of reliable post-functionalization of hexaphyrin derivatives, see: Suzuki, M.; Shimizu, S.; Shin, J.-Y.; Osuka A. Regioselective nucleophilic substitution reaction of meso-hexakis(pentafluorophenyl) substituted [26]hexaphyrin. *Tetrahedron Lett.* **2003**, *44*, 4597-4601. See also ref 18a.

[7] Lehn, J. M. Programmed Chemical Systems: Multiple Subprograms and Multiple Processing/Expression of Molecular Information. *Chem. Eur. J.* **2000**, *6*, 2097-2102.

[8] For reviews, see: (a) Ludlow, R. F.; Otto, S. Systems chemistry. *Chem. Soc. Rev.* **2008**, *37*, 101-108. (b) Goswami, A.; Saha, S.; Biswas, P. K.; Schmittel, M. (Nano)mechanical Motion Triggered by Metal Coordination: from Functional Devices to Networked Multicomponent Catalytic Machinery. *Chem. Rev.* **2020**, *120*, 125-199. (c) Benchimol, E.; Nguyen, B.-N. T.; Ronson, T. K.; Nitschke, J. R. Transformation networks of metal-organic cages controlled by chemical stimuli. *Chem. Soc. Rev.* **2022**, *51*, 5101-5135.

[9] [1.1.1.1.1.1]Hexaphyrins were discovered two decades ago independently by Cavaleiro and Osuka: (a) Neves, M. G. P. M. S.; Martins, R. M.; Tomé, A. C.; Silvestre, A. J. D.; Silva, A. M. S.; Félix, V.; Cavaleiro, J. A. S.; Drew, M. G. B. *meso*-Substituted Expanded Porphyrins: New and Stable Hexaphyrins. *Chem. Commun.* **1999**, 385-386. (b) Shin, J.-Y.; Furuta, H.; Yoza, K.; Igarashi, S.; Osuka, A. *meso*-Aryl-Substituted Expanded Porphyrins. *J. Am. Chem. Soc.* **2001**, *123*, 7190-7191.

[10] Optimized access to $(AB)_3$-type hexaphyrins has been described: Suzuki, M.; Osuka, A. Improved Synthesis of meso-Aryl-Substituted [26]Hexaphyrins. *Org. Lett.* **2003**, *5*, 3943-3946. For subsequent post-modification, allowing the straightforward formation of complex architectures, see ref 18a.

[11] Sankar, J.; Mori, S.; Saito, S.; Rath, H.; Suzuki, M.; Inokuma, Y.; Shinokubo, H.; Kim, K. S.; Yoon, Z. S.; Shin, J.-Y.; Lim, J. M.; Matsuzaki, Y.; Matsushita, O.; Muranaka, A.; Kobayashi, N.; Kim, D.; Osuka, A. Unambiguous Identification of Möbius Aromaticity for meso-Aryl-Substituted [28]Hexaphyrins(1.1.1.1.1.1). *J. Am. Chem. Soc.* **2008**, *130*, 13568-13579.

[12] For reviews, see: (a) Rzepa, H. S. Möbius Aromaticity and Delocalization. *Chem. Rev.* **2005**, *105*, 3697-3715. (b) Herges, R. Topology in Chemistry: Designing Möbius Molecules. *Chem. Rev.* **2006**, *106*, 4820–4842.

[13] Heilbronner, E. Hückel Molecular Orbitals of Möbius-Type Conformations of Annulenes. *Tetrahedron Lett.* **1964**, 5, 1923-1928.

[14] Calculated for *meso*-hexakis(pentafluorophenyl)[28]hexaphyrin: Kim, K. S.; Yoon, Z. S.; Ricks, A. B.; Shin, J.-Y.; Mori, S.; Sankar, J.; Saito, S.; Jung, Y. M.; Wasielewski, M. R.; Osuka, A.; Kim, D. Conformational Changes of meso-Aryl Substituted Expanded Porphyrins upon Protonation: Effects on Photophysical Properties and Aromaticity. *J. Phys. Chem. A* **2009**, *113*, 4498-4506.

[15] Mori, S.; Shimizu, S.; Taniguchi, R.; Osuka, A. Group 10 Metal Complexes of meso-Aryl-Substituted [26]Hexaphyrins with a Metal–Carbon Bond. *Inorg. Chem.* **2005**, *44*, 4127-4129.

[16] (a) Higashino, T.; Lim, J.; Miura, T.; Saito, S.; Shin, J.-Y.; Kim, D.; Osuka, A. Möbius Antiaromatic Bisphosphorus Complexes of [30]Hexaphyrins. *Angew. Chem. Int. Ed.* **2010**, *49*, 4950-4954. (b) Ishida, S.-i.; Tanaka, T.; Lim, J. M.; Kim, D.; Osuka, A. SiIV Incorporation into a [28]Hexaphyrin That Triggered Formation of Möbius Aromatic Molecules. *Chem. Eur. J.* **2014**, *20*, 8274–8278.

[17] Tanaka, T.; Sugita, T.; Tokuji, S.; Saito, S.; Osuka, A. Metal Complexes of Chiral Möbius Aromatic [28]Hexaphyrin(1.1.1.1.1.1): Enantiomeric Separation, Absolute Stereochemistry, and Asymmetric Synthesis. *Angew. Chem. Int. Ed.* **2010**, *49*, 6619-6621.

[18] (a) Ruffin, H.; Nyame Mendendy Boussambe, G.; Roisnel, T.; Dorcet, V.; Boitrel, B.; Le Gac, S. Tren-Capped Hexaphyrin Zinc Complexes: Interplaying Molecular Recognition, Möbius Aromaticity, and Chirality. *J. Am. Chem. Soc.* **2017**, *139*, 13847–13857. (b) Benchouaia, R.; Cissé, N.; Boitrel, B.; Sollogoub, M.; Le Gac, S.; Ménand, M. Orchestrating Communications in a Three-Type Chirality Totem. *J. Am. Chem. Soc.* **2019**, *141*, 11583-11593. (c) Boitrel, B.; Le Gac, S. Match–mismatch effects in two-fold transfer of chirality within a Möbius metalloreceptor. *Chem. Commun.* **2020**, *56*, 9166-9169. (d) Boitrel, B.; Le Gac, S. Interconversion between Möbius chiroptical states sustained by hexaphyrin dynamic coordination. *Chem. Commun.* **2021**, *57*, 3559-3562. (e) Ruffin, H.; Fihey, A.; Boitrel, B.; Le Gac, S. Möbius ZnII-Hexaphyrins Bearing a Chiral Coordinating Arm: A Chiroptical Switch Featuring P/M Twist Inversion Controlled by Achiral Effectors. *Angew. Chem. Int. Ed.* **2022**, *61*, e202113844.

[19] (a) Ménand, M.; Sollogoub, M.; Boitrel, B.; Le Gac, S. Hexaphyrin–Cyclodextrin Hybrids: A Nest for Switchable Aromaticity, Asymmetric Confinement, and Isomorphic Fluxionality. *Angew. Chem. Int. Ed.* **2016**, 55, 297–301. (b) Redox process: Suzuki, M.; Osuka, A. Reversible caterpillar-motion like isomerization in a N,N′-dimethyl hexaphyrin(1.1.1.1.1.1) induced by two-electron oxidation or reduction. *Chem. Commun.* **2005**, 3685-3687.

[20] (a) Basumatary, B.; Mitsuno, K.; Ishida, M.; Furuta, F. Bis-palladium(II) complex of doubly N-confused octaphyrin(1.1.1.1.1.1.1.1): Möbius aromaticity and chiroptical properties. *J. Porphyrins and Phthalocyanines* **2020**, *24*, 416-423. (b) Liang, K.; Chen, H.; Wang, X.; Lu, T.; Duan, Z.; Sessler, J. L.; Lei, C. Di-2,7-pyrenidecaphyrin(1.1.0.0.0.1.1.0.0.0) and Its Bis-Organopalladium Complexes: Synthesis and Chiroptical Properties. *Angew. Chem. Int. Ed.* **2023**, *62*, e202221277.

[21] Brandt, J. R.; Salerno, F.; Fuchter, M. J. The added value of small-molecule chirality in technological applications. *Nat. Rev. Chem.* **2017**, *1*, 0045.

[22] For reviews covering the field of chiroptical switches, see: (a) Feringa, B. L.; van Delden, R. A.; Koumura, N.; Geertsema, E. M. Chiroptical Molecular Switches. *Chem. Rev.* **2000**, *100*, 1789-1816. (b) Zhang, L.; Wang, H.-X.; Li, S.; Liu, M. Supramolecular chiroptical switches. *Chem. Soc. Rev*. **2020**, *49*, 9095-9120.

[23] Otto, S. An Approach to the De Novo Synthesis of Life. *Acc. Chem. Res.* **2022**, 55, 145-155, and references therein.

[24] These are similar to those of the related hexaphyrins with a single carboxylic acid arm, see ref 18e.

[25] The diastereotopic CH_2 protons in α position of the NH_2 function of the arm are well differentiated ($\Delta\delta$ = 1.05 ppm), in agreement with a conformational constraint imposed by the intramolecular coordination to zinc. *Inward* and *outward* binding of carboxylato and amino ligands, respectively, were also the preferred orientations in related systems with a carboxylate arm, see ref 18a,c-e.

[26] This difference of *meso* position of the arm *de facto* implies a *four-pyrrole isomerism* for the conversion of the Hückel antiaromatic complex to the Möbius aromatic one (Figure 1a), see also ref 18e.

[27] The combination of the two complementary systems requires both AcO^- and $BuNH_2$ achiral ligands that are *de facto* in competition with the carboxylate and amine functions of the arms. For ***(RR)*-11.Zn^{NH_2Bu}**, we previously found that it resists an excess of AcO^- (10 equiv., ref 18e). Concerning ***(S)*-10^{M}.Zn$_{OAc}$**, we observed herein that it resists well an excess of $BuNH_2$ (*ca.* 20 equiv., Figure S39), making it suitable for the envisioned study.

[28] Both their ^1H and ^{19}F NMR signatures are unaffected with respect to the complexes alone (Figure S41). The same results were obtained when $Zn(OTf)_2$ was added as the last ingredient. Besides, a competition experiment evidenced a higher affinity of zinc for the system ***(RR)*-11**/$BuNH_2$ compared to **6b**/AcO^- (Figure S42).

[29] Wu, A.; Isaacs, L. Self-Sorting: The Exception or the Rule? *J. Am. Chem. Soc.* **2003**, *125*, 4831-4835.

[30] This increasing is in agreement with the 1:0.7 ratio of the Δε values of the separated complexes, see Figure 4.

[31] Le Gac, S.; Marrot, J.; Jabin, I. Highly selective synthesis of a 1,3,5-tris-protected calix[6]arene type molecular platform through coordination and host-guest chemistry. *Chem. Eur. J.* **2008**, *14*, 3316-3322.